C: Surfaces, Interfaces, Porous Materials, and Catalysis

Bifunctional Behavior of a Porphyrin in Hydrogen-Bonded Donor-Acceptor Molecular Chains on a Gold Surface

Zhijing Feng, Simone Velari, Carlo Dri, Andrea Goldoni, Laerte L. Patera, Irene Regeni, Cristina Forzato, Federico Berti, Maria Peressi, Alessandro De Vita, and Giovanni Comelli

J. Phys. Chem. C, **Just Accepted Manuscript** • DOI: 10.1021/acs.jpcc.8b08939 • Publication Date (Web): 07 Mar 2019

Bifunctional Behavior of a Porphyrin in Hydrogen-Bonded Donor-Acceptor Molecular Chains on a Gold Surface

Zhijing Feng,[†,¶,1] Simone Velari,[‡,2] Carlo Dri,[†,¶,3] Andrea Goldoni,[Δ] Laerte L. Patera,[†,¶,4] Irene Regeni,[#,5] Cristina Forzato,[#] Federico Berti,[#] Maria Peressi,[†,∥,] Alessandro De Vita,[§,‡] and Giovanni Comelli[†,¶]*

[†] Department of Physics, University of Trieste, Via A. Valerio 2, I-34127 Trieste, Italy

[¶] TASC Laboratory, Istituto Officina dei Materiali IOM-CNR, S.S. 14 – km 163.5, I-34149 Trieste, Italy

[‡] Department of Engineering and Architecture, University of Trieste, Via A. Valerio 6/1, I-34127 Trieste, Italy

[Δ] Elettra-Sincrotrone Trieste, Area Science Park, S.S.14 – km 163.5, I-34149 Trieste, Italy

[#] Department of Chemical and Pharmaceutical Sciences, University of Trieste, via L. Giorgieri 1, I-34127 Trieste, Italy

[∥] DEMOCRITOS National Simulation Center, Istituto Officina dei Materiali IOM-CNR, via Bonomea 265, I-34136 Trieste, Italy

[§] King's College London, Department of Physics, Strand, London WC2R 2LS, United Kingdom

Abstract: Peculiar hydrogen-bonded molecular chains are spontaneously created from the self-assembly on a gold surface of a porphyrin functionalized with four aromatic amine moieties. The molecular chains are formed by a sequence of dyads, where the same molecule behaves alternately as a hydrogen bond acceptor or donor as a whole, at all its four aromatic amino groups. This remarkable bifunctional behavior is due to the conformational flexibility of the functionalizing amino groups, that switch from a planar, aniline-like conformation in donors, to a pyramidal, amine-like one in acceptors. Furthermore, we show that the acceptor porphyrins can trap gold adatoms underneath their center. Combined scanning tunneling microscopy (STM) experiments and density functional theory (DFT) calculations characterize the structural and electronic modifications suffered by such molecules to establish amino-amino interactions. Notably, scanning tunneling spectroscopy (STS) measurements show that the HOMO-LUMO gaps of the acceptors and donors are respectively larger and smaller with respect to the isolated molecule, according to the reduced extent of conjugation occurring in the acceptors. In summary, experimental and theoretical results reveal a remarkable hydrogen-bonded complex where the amino groups act both as hydrogen bond donors and acceptors and suggest how hydrogen bonding can modify the geometrical and potentially also the electronic structures of highly conjugated molecules.

1. Introduction

The exploitation of the functionalities of organic molecules is at the basis of new-concept electronic devices (such as OLEDs, biosensors) and could help to circumvent the drawbacks of the traditional technologies based on semiconductors, which are expected to reach their performance and miniaturization limit in the next few years. Among other molecules, porphyrin derivatives have attracted particular attention[1–4] because of their preeminent role in important biological processes such as light harvesting and oxygen transport. As organic semiconductors, porphyrins exhibit good stability and electronic transport properties. Porphyrins can be functionalized with a wide range of functional groups at their sides and metal atoms at their center, which can tailor their electronic properties and their self-assembly geometries.

Although many studies in literature have reported different properly functionalized porphyrins forming complexes through hydrogen,[5–7] covalent,[8–10] or metal-organic[6,11–14] bonds, the effect of the bonds on the electronic structure of the molecules has been poorly explored. Only recently, Chen *et al.*[10] have reported a study of the local electronic structure of a porphyrin in a covalent organic framework (COF) by showing how the HOMO-LUMO levels in the COF are shifted with respect to the single unbonded porphyrin.

Primary aliphatic amines (R-NH_2) have flexible geometry, can establish hydrogen bonds with each other, both as donors and acceptors, and can coordinate a metal atom.[15,16] Conversely, in solution and in crystalline structures, aromatic amines (Ar-NH_2) are usually found in a planar geometry and can act as hydrogen bond donors only, as their electron pair is involved in conjugation with the p system of the aromatic molecule.[17] This is the case, for instance of the amino groups of DNA nucleotides, which are involved only as donors in the recognition processes of Watson – Crick base pairing. The N-Au coordination bond has been used to form molecule-gold junction for single molecule conductance studies,[15,17–19] and it is characterized by a very fast charge transfer between

amines and gold substrates,[20] which makes this functionalization promising for potential applications in electronic devices. However, so far, except for self-assembled complexes in amino-carboxylic junctions,[21–23] the potential use of the amino-amino interaction for building supramolecular assemblies has been poorly explored.[16]

In this work, we present a peculiar donor-acceptor system formed on a gold surface from the self-assembly of an amino-functionalized porphyrin, the 5,10,15,20-tetra-(4-aminophenyl)-porphyrin (TAPP, **Figure 1a**). We chose to use a porphyrin with amino terminations for the properties mentioned above. Our combined STM experiments and DFT calculations reveal that the TAPPs form hydrogen-bonded chains via their amino-terminations by a donor-acceptor mechanism, despite the fact that the amino groups are aromatic. We show that aromatic amino groups can rearrange their structure to establish hydrogen bonds with each other and with the gold substrate, and that the acceptors usually trap gold adatoms at their center. Typical hydrogen-bonded systems are either formed by two (or more) different units (like the already mentioned DNA base pairing where aromatic amino groups always act as donors and oxygen carbonyl groups always act as acceptors) or by identical molecules where different atoms act as donor and acceptor (like in water and ice). Conversely, in our chains, each molecule behaves alternately as acceptor or donor as a whole. Furthermore, we investigated by STS the local electronic structure of the chains revealing larger and smaller HOMO-LUMO gaps of the acceptor and donor TAPPs, respectively, with respect to the single isolated TAPP. Our results present a unique hydrogen-bonded complex and provide insight on the role of hydrogen bonds in the modification of the geometrical and electronic structures of molecules. Moreover, the reported structure represents, to our knowledge, a unique example of hydrogen bonding involving aromatic amine nitrogen groups as acceptors.

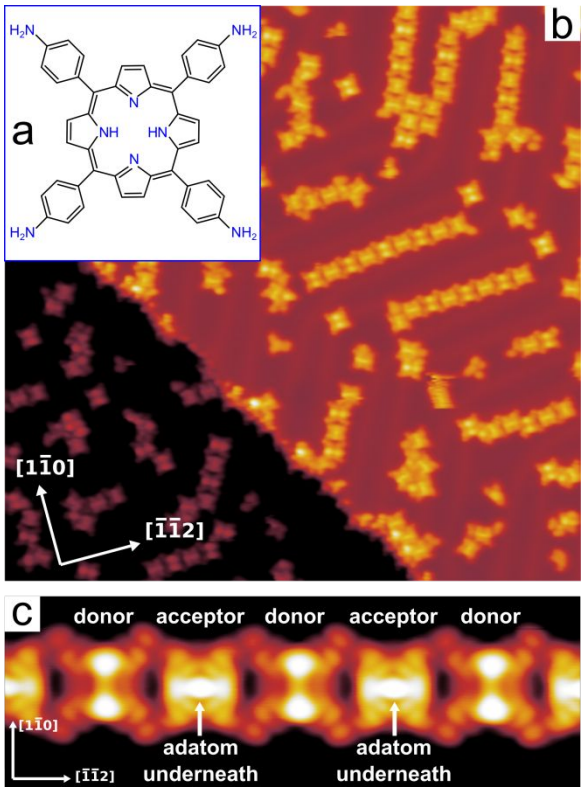

Figure 1. (a) Chemical structure of 5,10,15,20-tetra-(4-aminophenyl)-porphyrin (TAPP). (b) TAPP chains on Au(111), the maximum length of these chains being limited by the herringbone reconstruction of the surface. (c) High-resolution image of a TAPP chain, where the alternated appearance (due to the donor-acceptor alternation) of the molecules is evident. "Bright" TAPPs have a bright feature at their center, likely due to the presence of a gold adatom underneath the molecule. Image parameters: (b) V= -1.0 V, I = 0.05 nA, 50×50 nm^2; (c) V= -1.0 V, I = 0.3 nA, 10×3 nm^2.

2. Methods

2.1 Experimental Method

Experiments were performed in UHV conditions at a base pressure of 1×10^{-8} Pa. 5,10,15,20-tetra(4-aminophenyl)porphyrins (abbreviated TAPP, PorphyChem, purity 98%) were evaporated from a Knudsen cell at 520 – 570 K on a clean monocrystalline Au(111) sample at room temperature. The

Au(111) sample was previously cleaned via standard Ne^+ ion sputtering followed by annealing to 870 K for 10 minutes. STM imaging was performed with an Omicron Low Temperature STM, working at ~ 4.3 K. Images were acquired in the constant current mode, with the bias voltage applied to the sample and the tip at ground. Electrochemically etched tungsten tips were used for imaging.

2.2 Theoretical Method

DFT calculations were performed with the plane-wave pseudopotential package QUANTUM ESPRESSO (QE)[24] using GGA-PBE[25] ultrasoft pseudopotentials.[26] The wave function energy cut-off was set at 408 eV. Considering the large size of the cell, the Brillouin zone sampling included only the Gamma point. Since van der Waals interactions play a non-negligible role in self-assembled organic structures, the calculations were performed including the semi-empirical dispersion-corrected DFT (DFT-D) method proposed by Grimme,[27] implemented in the QE package[28] and already used by us in a previous publication to successfully study the gold adatom stabilization by dimethyl sulfoxide on Au(111).[29]

The Au(111) surface was modeled with a three-layer slab for the simulations of the single TAPP molecule adsorption and only two layers for the chain, allowing in both cases a vacuum spacing of ≈ 1.4 nm. For the single TAPP adsorption, the bottom layer of the slab was kept fixed at the bulk Au calculated structure (lattice parameter a_{bulk}=0.407 nm, equal to the experimental one) to mimic the behavior of the metal substrate. For the chain model, the two gold layers were kept fixed, except for the gold atoms underneath the center of the two porphyrins. The forces were relaxed up to 0.26 eV/Å. STM images were simulated within the Tersoff-Hamann approximation[30] using the energy-integrated local density of states (ILDOS) and mapping its iso-surfaces to simulate the experimental "constant current" condition. The images were simulated at various biases, at an ILDOS value for the iso-surface of 4×10^{-3} nm^{-3}, lying at an average distance of approximately 0.5 nm from the outmost atomic layer.

3. Results and discussion

Figure 1b shows an STM image of TAPP molecules deposited on Au(111), where they form chains along the herringbone reconstruction[31] of the substrate, which limits their length. A closer look at these chains in **Figure 1c** raises questions concerning the interaction linking TAPPs in a chain, and more specifically, the reason why the units along the chain, which are identical TAPP molecules, display alternate appearance in the STM images. We point out that such alternated appearance contrast of TAPPs is imaging bias-dependent: at low bias voltage the alternated contrast is present, but it is weaker (see **Figure S1**).

To answer these questions, we performed DFT simulations on this system and compared them with our experimental results. First, a single TAPP was modeled in the gas phase and on the Au(111) surface (see Supporting Information, **Figure S2** and **S3**). In the gas phase, our DFT results suggest that the most stable geometry is characterized by a saddle-shaped macrocycle with the two pairs of opposite pyrroles tilted by 15° degrees in different directions, and the phenyl rings alternately twisted by 46° degrees with respect to the molecular plane. The presence of the two inner H atoms does not alter the inclination of the pyrroles (**Figure S2**). Conversely, when the molecule is adsorbed on the surface, two different conformations are possible. We call κ-pyrroles the two opposite pyrrole rings with N atoms tilted upwards (following the notations of Seufert *et al.*[32]), and α-pyrroles those tilted downwards, respectively (see **Figure S3**). The two different conformations of the isolated adsorbed TAPP are characterized by the two inner hydrogens located on the α-pyrroles (conformation saddle-A) or κ-pyrroles (conformation saddle-B). The twisting angle of the aminophenyl terminations is 20 degrees, strongly reduced with respect to the gas phase, while the coordination geometry of the N atoms of the amines is halfway between planar and tetrahedral. The inclination of the α-pyrroles is strongly increased (see **Figure S3** for details). The two conformations are very close in energy, with saddle-A slightly favored by 0.22 eV. The simulated

STM images shown in **Figure S3e** are practically indistinguishable from each other, since the inner hydrogens are little visible, and both conformations are compatible with experiments where TAPPs are in monolayer phase ("dark" molecules in **Figure S4a)** or a single TAPP molecule is imaged (**Figure S4b**). We point out that the saddle-shaped macrocycle and the tilted phenyls are typical geometries of tetraphenylporphyrins in gas phase or adsorbed on metal surfaces, as widely reported in the literature.[32–36] The recent work of Chen *et al.*[10] also reports a saddle-shaped TAPP macrocycle on Au(111) (equivalent to our saddle-A) obtained from DFT calculations, but, surprisingly, a planar conformation for the free-standing molecule.

For the TAPP chains, we expected that some hydrogen bonds between the amino terminations of TAPPs are linking the molecules. Indeed, the possibility to separate the TAPPs from the chains by STM manipulation (**Figure S5**) suggests that weak interactions between the molecules drive the chain formation. We cannot exclude a possible role played by the Au(111) herringbone reconstruction in facilitating the formation of the chains; in any case, since tetraphenylporphyrins without amino-terminations do not align along the herringbone reconstruction and do not form chains,[37] the amino terminations of the TAPPS must have an active role in the process. We simulated an ideal endless TAPP chain on Au(111) using the smallest periodically repeated unit cell commensurate with the substrate and compatible with the experimental chain period (cell period of $3\sqrt{6}\ a_{bulk}$ = 3.00 nm along the $[\bar{1}\bar{1}2]$ direction, slightly smaller than the experimental one of 3.30 ± 0.20 nm), containing two adjacent TAPP molecules close to each other. We performed also the simulation with the next larger commensurate unit cell (cell period of $3.5\sqrt{6}\ a_{bulk}$ = 3.5 nm) which we excluded since it resulted in no chain formation, with each of the two TAPP molecules relaxing to the isolated molecule geometry. We tested several conformations, involving different orientations of the TAPP molecules, and none of them yielded a good match between the simulated and experimental STM images. In particular, the alternate appearance of the porphyrins in **Figure 1c** could not be reproduced in the simulations.

We thus hypothesized the alternate presence of a gold adatom underneath the center of TAPPs in a chain, suggested by the well-known fact that native gold adatoms on Au(111) can detach from surface steps and diffuse across the surface terraces[38–40] where they can interact with ligands such as cyano (CN) groups,[14,41–44] thiols,[45,46] or even small solvents.[29] Indeed, in two recent works, Mielke *et al.*[37] and Pham *et al.*[47] demonstrated that gold adatoms can be trapped underneath porphyrins on Au(111), both spontaneously and by STM manipulation. In their STM images, Mielke *et al.* find two types of porphyrins, "bright" ones and "dark" ones, and they show that the "bright" porphyrins have a gold adatom underneath. This is similar to what we observe in both TAPP chains (**Figure 1c**) and compact phases at high coverage (**Figure S4a**). We point out that at coverage above 0.5 monolayers, TAPPs change their self-assembly from molecular chains to a compact phase. Since the latter process involves just adding more molecules at room temperature on the surface, the "bright" TAPPs in the chain and in the compact phase, having the same appearance in the STM images, must be the same type of molecule. Furthermore, the "bright" TAPPs resemble the TAPPs at surface steps (**Figure S4b**), where it is more likely for the porphyrins to have adatoms underneath, being next to the source of the adatoms.[38]

Therefore, we placed a gold adatom underneath one of the two adjacent TAPP molecules on Au(111) in our model and compared several possible conformations combining saddle-A and saddle-B TAPPs, in any case with an alternated perpendicular orientation of the macrocycle (see **Figure S6**). This was suggested by the STM image in **Figure 1c**, where the couple of bulge features visible at the sides of each molecule was taken as an indication of the alternated perpendicular orientations of the protruding α-pyrroles, on the basis of the simulations reported in **Figure S3**. Our resulting best model (shown in **Figure 2a-c**), yielding the energetically most stable structure and the simulated STM images that best match the experimental ones, is obtained by placing two saddle-B TAPPs (one with adatom, the other without) perpendicular to each other, meaning that the lines connecting the opposite κ-pyrroles inside each of the two saddle-TAPPs are perpendicular. Upon

relaxation, the two molecules have a geometry similar to the isolated saddle-B TAPP, apart from a small uniform compression along the chain for the one with κ-pyrroles aligned in that direction, which changes its global shape from square to rectangular. In the chain, the aminophenyl terminations are tilted into a conformation that favors the interaction of amino groups of two neighboring molecules. Upon DFT relaxation, the coordination geometry of the N atom of the amine, which in the isolated saddle TAPP is halfway between planar and tetrahedral (zoomed model in **Figure S3d**), becomes more tetrahedral in the acceptor amine and flatter in the neighbor donor amine (zoomed model in **Figure 2c**). This geometry favors the interaction of the lone pair of the N atom of the acceptor amine (hydrogen bond acceptor) with a hydrogen of the donor (hydrogen bond donor), with the formation of an amino-amino hydrogen bond. The four amino groups of a TAPP must have the same behavior since they all have the same appearance in the STM images and indeed our DFT model confirms such symmetry. Thus, in the TAPP chain, each molecule behaves alternately as acceptor (**Figure 2**, left) or donor (**Figure 2**, right) of hydrogen bond as a whole, with the acceptor trapping a gold adatom underneath. The simulated STM image of this model (**Figure 3a**) closely resembles the experimental one (**Figure 1c**).

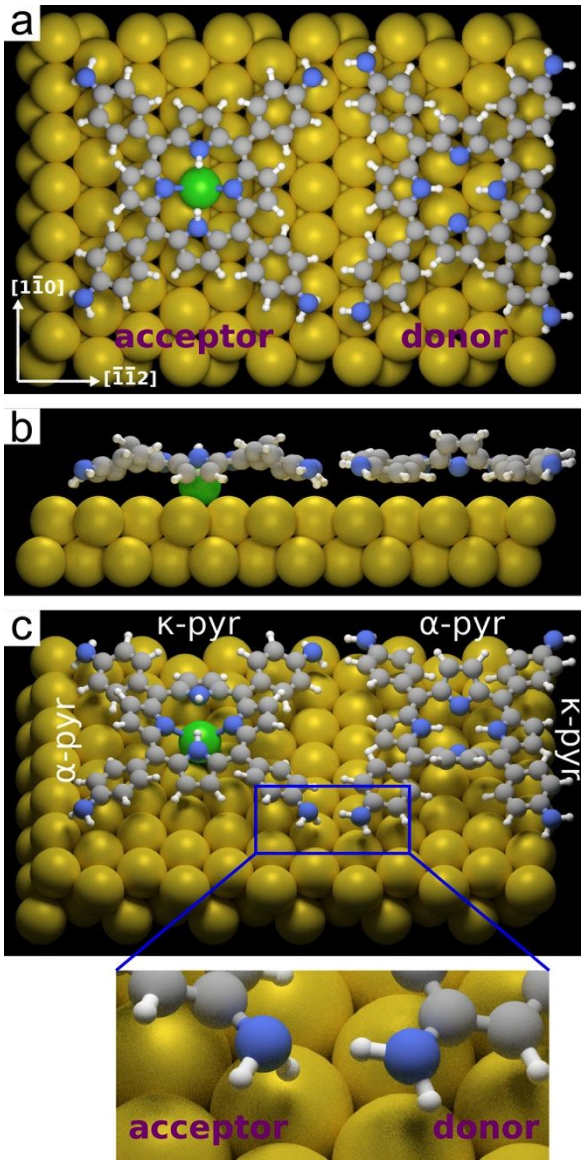

Figure 2. (a) Top view, (b) side view and (c) perspective view of the stick and ball model of a TAPP chain on Au(111) obtained by DFT. The unit cell is periodically repeated along the [$\bar{1}\bar{1}$2] direction. The saddle shape of the acceptor and donor in the present model is essentially the same of the TAPP saddle-B, apart from a small squeezing of the donor along the direction of the chain and a small rearrangement of the geometry of the amino groups responsible of the intermolecular interaction along the chain. A zoomed image of the (c) perspective view highlights the donor-acceptor scheme of the aminophenyl terminations. The gold adatom trapped by the acceptor is painted in green to ease its identification. In panel c the κ-pyrroles and α-pyrroles are labeled κ-pyr and α-pyr, respectively, with the inner hydrogens always located on the two κ-pyrroles. Notice the

"orthogonal" disposition of the acceptor with respect to the donor, meaning that the lines connecting the opposite κ-pyrroles inside each of the two saddle-TAPPs, i.e., the orientations of the macrocycles, are perpendicular.

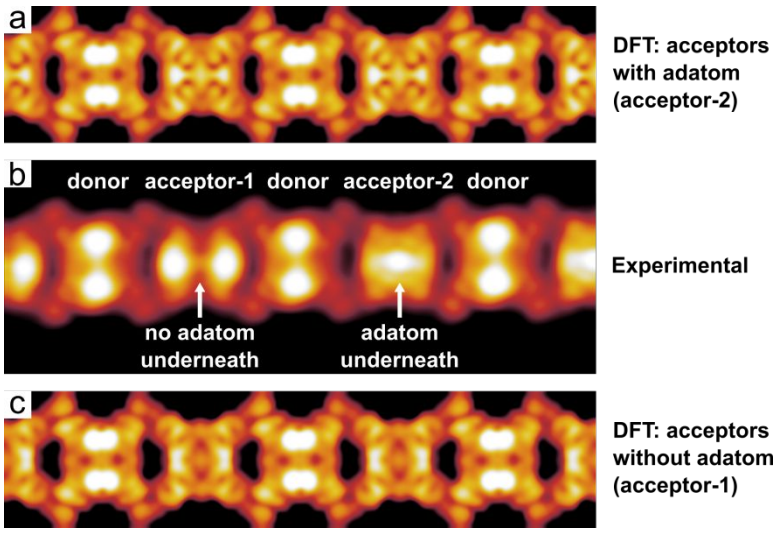

Figure 3. Comparison of an experimental STM image with the simulated ones. (a) Simulated STM image of the model with the acceptors including an adatom at their center (acceptor-2). (b) Experimental image (V = -1.0 V, I = 0.2 nA, 10×3 nm^2) of a TAPP chain showing an acceptor-1 and an acceptor-2. (c) Simulated STM image of the model with the acceptors without adatom at their center (acceptor-1).

The donor-acceptor TAPP interaction is visualized in **Figure S7**, which shows the electron density rearrangement calculated in a chain where neither the trapped Au adatom nor the substrate are present, to focus on the amino groups: the polarization in the sequence N(acceptor)···H-N(donor) of the amino-amino group is the typical polarization of a hydrogen bond (red/blue: excess/depletion of electrons). The calculated atomic projected charges indicate that the donor TAPP has about 0.4 electrons more than the acceptor. **Figure S8** refers to a situation where both the substrate and the

Au adatom have been put back in place: on average each TAPP gives more than one electron to the gold substrate, and the acceptor TAPP trapping the adatom now has about 0.4 electrons more than the donor TAPP. These findings suggest that, while the acceptor TAPP loses electrons to the donor through the amino-amino interaction, it gains electrons from the substrate, also via the amino-gold interaction (**Figure 2** and **S8**). Remarkably, the N atom of the aminophenyl groups appears to be able to rearrange its coordination geometry relative to its gas phase structure in order to interact with the substrate and its neighbor molecules. This behavior is unknown, to our knowledge, also in the solid state, and a query on the Cambridge Crystallographic Data Centre for X-ray structures containing the aminophenyl moiety gave no results showing the nitrogen group acting as a hydrogen bond acceptor, while the amino group was acting as the donor in almost all the structures.[48]

To experimentally confirm the presence of the adatoms underneath the acceptors, we also carried out manipulation experiments similar to those performed by Mielke *et al.*[37] They firstly pulled a single tetraphenylporphyrin from the elbow of the herringbone reconstruction, revealing the presence of an adatom underneath, and secondly pushed the molecule back onto the elbow, restoring the original appearance of the porphyrin. Our attempts to pull single TAPP molecules, sitting on the herringbone elbows, away from their position were unsuccessful: the molecules can be rotated but not moved aside. This suggests that TAPP binds its adatom more strongly than tetraphenylporphyrin. Indeed, as mentioned above, far from the herringbone elbows, we can easily move the acceptors, with the molecules always maintaining their original appearance, suggesting that the adatom is strongly bound to the molecule and moves with it on the surface (**Figure S5**). From the elbow, instead, the TAPP cannot be moved because it is strongly bound to the adatom which, in turn, is strongly bound to the substrate. Mielke *et al.* could perform successfully their manipulation experiments only for molecules sitting at the herringbone elbows, where the adatom is strongly bound to the substrate, while after moving tetraphenylporphyrins with adatom sitting in

other positions they could not find any adatom below because it was lost. The different behavior can be rationalized considering that, in our case, the acceptor TAPP sits centrally above the adatom and binds it through its internal N-atoms, while in Mielke *et al*.'s work, the tetraphenylporphyrin sits asymmetrically on the adatom (it appears asymmetric in the STM images). Therefore, we conclude that the amino-terminations help the TAPP molecule to bind more strongly the adatom underneath. We tried also the reverse experiment by creating adatoms on the surface and then pushing a single TAPP molecule on the adatom: these experiments were unsuccessful because the amino-terminations always bind the adatom before the TAPP can go above it.

We also stress that in our model the acceptors trap one gold adatom underneath by coordination bond through the N atoms of their α-pyrroles (**Figure 2**), but they do not metalate. The metalation process of porphyrins has been widely studied in the literature, especially their self-metalation on metal surfaces, such as Cu, Fe or Ni,[49–54] and their direct metalation by evaporating metal atoms on the surface.[55–57] However, to our knowledge, in the literature, no study of spontaneous metalation of porphyrins with gold atoms on surfaces has been reported up to now, likely because the size of gold atom prevents their spontaneous metalation. Indeed, the simulated STM image of the model in which the acceptor is metalated (**Figure S9**) has a poorer matching with the experimental image. Furthermore, from our DFT calculations we exclude also the possibility that the adatom may be sitting above the center on the TAPP: when we place it there, upon DFT relaxation it moves spontaneously below the porphyrin. Pham *et al.*[47] and Bischoff *et al.*[58] reported "manual" metalation of porphyrins with single adatoms by applying voltage pulses with the STM tip onto single porphyrins. We tried to perform the same sequence of STM manipulation experiments on our TAPPs in chains, but the high voltage pulses required for manipulating the acceptors-2 disassemble the chains. However, by exploiting the FAST module developed in our laboratory[59–61] we verified that above room temperature the gold adatoms can diffuse underneath the TAPPs in the compact monolayer phase, in accordance with recently published literature.[62] Indeed, as shown in **Figure**

S10, during the acquisition of a high speed sequence of STM images, several molecules switch on and/or off (changing their appearance from bright to dark and viceversa), suggesting that gold adatoms are diffusing underneath the TAPP molecules, which therefore cannot be metalated. As mentioned above, as the acceptor-2 in the chains (and also when it is separated from the chain, **Figure S5**) must be the same type as the bright TAPPs in the compact monolayer, this argument can be used to rule out metalation of the acceptor-2.

TAPP chains like the one showed in **Figure 1c** and modeled in **Figure 2** are by far the most common imaged on the surface, but exceptions can be found. **Figure 3b** shows an experimental STM image of a TAPP chain where two acceptors have different appearances: the first one, named acceptor-1, appears like its neighbor donor TAPPs after 90° rotation, while the second one, named acceptor-2, strictly resembles the acceptor TAPPs in **Figure 1c**. Most of the acceptors found on the sample are similar to the acceptor-2, with a bright protrusion at their center, while acceptors-1, without bright protrusion, are rarely found. The simulated STM image (**Figure 3c**) of a TAPP chain model where the acceptors have no trapped adatoms underneath well reproduces acceptors-1. The corresponding model is practically the same as the one in **Figure 2**, just without adatom underneath the acceptor. This finding further supports our adatom hypothesis: the bright protrusion at the center of the acceptors-2 is likely associated with the presence of a gold adatom underneath each of them, which we found to be necessary to reproduce the experimental images in **Figure 1c**, especially the bright feature at the center of the acceptor-2. We point out that the appearance of the donors and all the aminophenyl groups in **Figure 3a, c** is also in good agreement with the experimental images: In particular, the pairs of bright features visible in both the experimental and simulated images at the sides of each donor and acceptor are associated with the α-pyrroles.

It remains to discuss whether it is the formation of the TAPP chains that leads to the trapping of an adatom by the acceptors or vice versa. On the one side, the interaction between molecules within a chain seems to be weaker than the interaction between macrocycle and adatom (**Figure S5**) and we

find single TAPPs with adatom (**Figure 1b**), which would suggest that the trapping of the adatom comes first, thus leading then to the chain formation. On the other side, since most of the acceptors and none of the donors are found to trap adatoms, we can hypothesize that the geometrical conformation of the acceptors in the chains, characterized by a slightly more spacious tetrapyrrole cage than the donors, favors trapping of gold adatoms. Indeed, according to our models, the structure of the acceptors remains essentially the same with or without an adatom located underneath. Conversely, donors in the chain undergo a small squeezing along its direction, reducing the space inside their macrocycles and thus preventing the trapping of adatoms underneath their center (see **Table S1**). In addition to pure steric arguments, a different charge distribution between acceptor and donor TAPPs could also explain their different behavior with respect to adatoms trapping. In a recent paper, Lepper *et al.*[63] reported that the cyano-terminations on a tetraphenylporphyrin reduce the self-metalation rate of the molecules on Cu(111). By a combination of STM experiments and DFT calculations, Lepper *et al.* showed that the cyano-terminations draw charge from the Cu substrate to the porphyrin. As a consequence, the latter switches to an inverted saddle-shape geometry and reduces the self-metalation rate. Even though the TAPPs don't undergo metalation, a similar mechanism might explain the peculiar behavior of donor TAPP, where the charge drawn from the neighboring acceptors by its amino-terminations could induce a change in the macrocycle geometry. We could argue whether the alternating trapping of a gold adatom by donors and acceptors in the chain is related to a different position of their centers. From the experimental side, it is very difficult to obtain specific information regarding the position of each molecule with respect to the substrate. From DFT simulations, after the optimization of the atomic positions which allows also translational displacements of the chain with respect to the surface, the centers of both donor and acceptor sit onto a hollow site (**Figure 2**), which can potentially accommodate an adatom. A slightly different period (like the next larger period of $7\sqrt{6}/2\ a_{\mathrm{bulk}} \sim$ 3.5 nm commensurate with the substrate) could correspond to donor and acceptor centered in non-equivalent surface sites, thus favoring the trapping of an adatom by one TAPP rather than by the

other (**Figure S11**). However, we cannot confirm this picture, since, as previously mentioned, DFT simulations performed using the larger unit cell resulted in no chain formation. Summarizing, we have elements that point to both directions and therefore cannot provide a conclusive solution to the dilemma. In any case, as mentioned above, the main point of our discussion - the amino terminations of the TAPPs are crucial for the formation of the molecular chains since tetraphenylporphyrins without amino-terminations do not form chains[37] - remains valid.

We also performed STS on the TAPPs along the chain to investigate their electronic structure. As shown in the normalized *dI/dV* spectra in **Figure 4**, for TAPPs chains we observe that the HOMO and LUMO peaks of the acceptors-2 and donors are significantly shifted with respect to the isolated TAPP. The HOMO (-0.40 eV) and LUMO (+1.40 eV) energies of the single isolated TAPP are compatible with the values found by Chen *et al.*[10] The acceptor-2 has its HOMO (-0.70 eV) and LUMO (+1.55 eV) levels shifted to lower and higher energy, respectively, and therefore a larger HOMO-LUMO gap (2.25 eV) with respect to the single TAPP one (1.80 eV). Conversely, the donor has a smaller gap (1.35 eV), with both its HOMO (-0.85 eV) and LUMO (+0.50 eV) peaks shifted to lower energy with respect to the single TAPP. The bigger HOMO-LUMO gap of the acceptor-2 and the smaller HOMO-LUMO gap of the donor with respect to the single TAPP are in agreement to the reduced extent of conjugation occurring in the acceptors. We tried to acquire also STS spectra on acceptor-1, but because of poor statistics (too few acceptor-1 molecules on the surface) and unstable STS condition, likely due to chemical reactions such as deprotonation or tautomerization,[64,65] we could not obtain a reliable set of spectra for acceptor-1. We also observe that, at variance with the present results, Mielke *et al.*[37] and Pham *et al.*[47] found that tetraphenylporphyrins with adatom trapped underneath or metalated tetraphenylporphyrins have their STS spectrum rigidly shifted towards occupied states with respect to those without adatom. However, a direct comparison between our results and those of Mielke et al.[37] and Pham et al.[47] is not appropriate, since, whereas in the latter cases the tetraphenylporphyrins are mostly isolated and

differ only for the presence of an adatom, our TAPPs belong to chains and differ also for being in a donor or acceptor state. DFT calculations of the electronic density of states (DOS) give a TAPP HOMO-LUMO gap of 1.2 eV, almost independent on the specific conformation, and an almost rigid energy shift of about 0.3 eV toward occupied states for the acceptor-2 with respect to the donor in the chain. This result is similar to that reported by Mielke *et al.*[37] and Pham *et al.*[47] when adding an adatom below a porphyrin. Therefore, we can conclude that the DFT calculated DOS correctly account for the effects related to the presence of the trapped adatom, but do not explain adequately all the features of the STS spectra of the TAPP chains. In addition to the limitation of DFT in describing the unoccupied electronic states, a possible reason could be our simplified chain model, whose periodicity, as mentioned above, is forced to match the one of the substrate in the smallest possible simulation cell compatible with the experiment. This choice sets some constraints on the donor and acceptor shape and on their relative registry with respect to the Au(111) substrate, whose details could be relevant in the description of space and energy resolved quantities like the local DOS. In conclusion, our STS results show that the hydrogen bond is responsible for the HOMO-LUMO gap decrease in the donors and increase in the acceptors-2 with respect to the isolated TAPP. We point out that, since we could not compare the STS spectra of acceptor-2 with acceptor-1 due to lack of data, we do not have a clear evidence of the effect of the hydrogen bond in the HOMO-LUMO gap modification in the acceptors with or without a trapped adatom. However, it is likely that the hydrogen bond plays a relevant role, since we know from literature that the adatom is responsible for only a rigid shift of the HOMO and LUMO peaks, without affecting the gap.

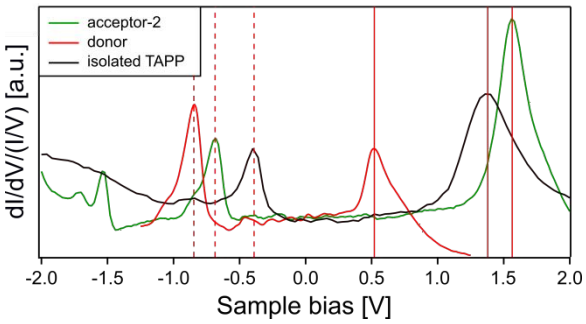

Figure 4. *dI/dV* (normalized to *I/V*) spectra acquired at the center of the acceptor-2 (green), the donor (red) in a chain, and onto an isolated single TAPP without adatom (black). Dashed red vertical lines indicate the HOMO, while red vertical lines indicate the LUMO. With respect to the isolated TAPP (HOMO = -0.40 eV, LUMO = +1.40 eV): the acceptor-2 has its HOMO (-0.70 eV) and LUMO (+1.55 eV) shifted to lower and higher energy, respectively, giving thus a wider energy gap of 2.25 eV. The donor has both its HOMO (-0.85 eV) and LUMO (+0.50 eV) peaks shifted to lower energy and a smaller energy gap of 1.35 eV. The states between the HOMO-LUMO peaks of TAPPs are associated to the Au(111) substrate.

Finally, we verified the stability of the TAPP chains on Au(111) by annealing the sample to increasing temperatures. Isolated TAPP molecules appear to be stable up to ~ 520 K, while undergo chemical modification (cyclodehydrogenation) at higher temperatures, assuming a mostly flat rectangular-shaped configuration, as reported by Di Santo *et al.*[66] (see **Figure S12**). Since these cyclodehydrogenated TAPPs feature a bright spot at their center (at least at a bias of -1.0 V), we hypothesize that they might be metalated due to the high annealing temperature (**Figure S12**). As to the TAPP chains on Au(111), we performed STM imaging also at 77 K and room temperature. At 77 K the images have a similar appearance as at 4 K, but they are fuzzy because the chains can move under the effect of the STM tip electric field. At room temperature, it is impossible to image the chains, since the molecules are very mobile on the surface, while, on the contrary, a compact monolayer can still be imaged above room temperature (see also **Figure S10**, where T=373 K).

Since we need to cool down the sample to at least 77 K to obtain STM images, we do not have clear information on the stability of the TAPP chains above 77 K, as we cannot exclude that they form during the cooling down process in the STM. Summarizing, the TAPP molecules are stable on Au(111) up to 520 K, while the chains are stable till at least 77 K.

4. Conclusions

To summarize, in the present work, we have studied a unique hydrogen-bond donor-acceptor complex formed from the self-assembly of an aminophenyl-functionalized porphyrin (TAPP) on Au(111). Our combined experimental STM images and DFT calculations demonstrated that the TAPP molecules, via amino-amino interactions of their terminations, form chains on Au(111), where each TAPP behaves alternately as a hydrogen bond donor or acceptor as a whole. We have shown that the amine functional groups can undergo a significant rearrangement, with their N atoms modifying their coordination geometry from planar to tetrahedral, to establish the hydrogen bonds with their neighbors. Moreover, in the STM images most of the acceptors have a bright protrusion at their center (acceptor-2), which we demonstrated by STM experiments and DFT calculations that can be associated to a gold adatom located just below their center. The *dI/dV* spectra show a bigger HOMO-LUMO gap of the acceptor-2 and a smaller HOMO-LUMO gap of the donor with respect to the single TAPP, in accordance with the reduced extent of conjugation occurring in the acceptors. Our alternated donor-acceptor chain is a remarkable complex because it is generated from the self-assembly of a single molecule and our results provide insight on how hydrogen bonds can induce modifications in the geometrical and potentially also in the electronic structures of molecules.

ASSOCIATED CONTENT

Supporting Information Description

Supporting Information is available is available free of charge on the ACS Publications website at DOI: 10.1021/**********

DFT results: models of the single TAPP in the gas phase and adsorbed on Au(111) (saddle-A and saddle-B TAPP) and of alternative conformations of the TAPP chain (with different combination of saddle-A and saddle-B molecules with trapped gold adatoms, and with metalated acceptor); simulated STM images of saddle-A and saddle-B TAPP; plots of the calculated electronic density rearrangement upon bonding between adjacent molecules in the chain and between the chain and the substrate; Au(111) substrate model with periodicity explained. Experimental STM images of TAPP chains in a large area at different bias; TAPP molecules in compact monolayer phase and at surface steps; STM manipulation experiments on TAPP chains; FAST-STM image sequence of a compact TAPP monolayer with adatoms diffusing below.

AUTHOR INFORMATION

Corresponding Author

* E-mail: (M.P.) peressi@ts.infn.it

ORCID

Zhijing Feng: 0000-0002-8778-8878

Carlo Dri: 0000-0001-9040-5746

Andrea Goldoni: 0000-0001-9989-3889

Laerte L. Patera: 0000-0002-6214-5681

Cristina Forzato: 0000-0003-4213-9089

Federico Berti: 0000-0001-5608-3798

Maria Peressi: 0000-0001-6142-776X

Alessandro De Vita: 0000-0002-3912-5375

Giovanni Comelli: 0000-0003-4603-2094

Present Addresses

[1] Z.F.: Department of Chemical Engineering and Materials Science, University of California, Irvine, Irvine, CA 92697, USA

[2] S.V.: Modefinance, AREA Science Park, Località Padriciano 99, I-34149 Trieste, Italy

[3] C.D.: ELETTRA-Sincrotrone Trieste, S.S. 14 km 163.5, Basovizza, I-34149 Trieste, Italy

[4] L.P.: Institute of Experimental and Applied Physics, University of Regensburg, D-93053 Regensburg, Germany

[5] I.R.: Department of Chemistry and Chemical Biology, TU Dortmund University, Otto-Hahn-Strasse 6, 44227 Dortmund, Germany

Author Contributions

The manuscript was written through contributions of all authors. All authors have given approval to the final version of the manuscript.

Notes

The authors declare no competing financial interest.

ACKNOWLEDGMENTS

M.P. and G.C. acknowledge the University of Trieste through the program "Finanziamento di Ateneo per progetti di ricerca scientifica – FRA 2015". Computational resources have been obtained from the CINECA Consortium through the ISCRA initiative and the agreement with the University of Trieste. A.D.V. acknowledges further support by the EPSRC HEmS Grant No. EP/L014742/1 and by the European Union Horizon 2020 research and innovation program (Grant No. 676580, The NOMAD Laboratory, a European Centre of Excellence) and is grateful to the UK Materials and Molecular Modelling Hub for computational resources, which is partially funded by EPSRC (EP/P020194/1). A.G. acknowledges by the NATO – G51 project.

During the final editing of the present article, our dear colleague and friend Alessandro De Vita tragically passed away due to a road accident. We dedicate this work to his loving memory.

References

(1) Auwärter, W.; Écija, D.; Klappenberger, F.; Barth, J. V. Porphyrins at Interfaces. *Nat. Chem.* **2015**, *7*, 105–120.

(2) Jurow, M.; Schuckman, A. E.; Batteas, J. D.; Drain, C. M. Porphyrins as Molecular Electronic Components of Functional Devices. *Coord. Chem. Rev.* **2010**, *254*, 2297–2310.

(3) Grätzel, M. Dye-Sensitized Solar Cells. *J. Photochem. Photobiol. C Photochem. Rev.* **2003**, *4*, 145–153.

(4) Hagfeldt, A.; Boschloo, G.; Sun, L.; Kloo, L.; Pettersson, H. Dye-Sensitized Solar Cells. *Chem. Rev.* **2010**, *110*, 6595–6663.

(5) Yokoyama, T.; Yokoyama, S.; Kamikado, T.; Okuno, Y.; Mashiko, S. Selective Assembly on a Surface of Supramolecular Aggregates with Controlled Size and Shape. *Nature* **2001**, *413*, 619–621.

(6) Fendt, L.-A.; Stöhr, M.; Wintjes, N.; Enache, M.; Jung, T. A.; Diederich, F. Modification of Supramolecular Binding Motifs Induced By Substrate Registry: Formation of Self-Assembled Macrocycles and Chain-Like Patterns. *Chem. - A Eur. J.* **2009**, *15*, 11139–11150.

(7) Yokoyama, T.; Kamikado, T.; Yokoyama, S.; Mashiko, S. Conformation Selective Assembly of Carboxyphenyl Substituted Porphyrins on Au (111). *J. Chem. Phys.* **2004**, *121*, 11993–11997.

(8) Grill, L.; Dyer, M.; Lafferentz, L.; Persson, M.; Peters, M. V; Hecht, S. Nano-Architectures by Covalent Assembly of Molecular Building Blocks. *Nat. Nanotechnol.* **2007**, *2*, 687–691.

(9) Lafferentz, L.; Eberhardt, V.; Dri, C.; Africh, C.; Comelli, G.; Esch, F.; Hecht, S.; Grill, L. Controlling On-Surface Polymerization by Hierarchical and Substrate-Directed Growth. *Nat.*

Chem. **2012**, *4*, 215–220.

(10) Chen, C.; Joshi, T.; Li, H.; Chavez, A. D.; Pedramrazi, Z.; Liu, P.-N.; Li, H.; Dichtel, W. R.; Bredas, J.-L.; Crommie, M. F. Local Electronic Structure of a Single-Layer Porphyrin-Containing Covalent Organic Framework. *ACS Nano* **2018**, *12*, 385–391.

(11) Heim, D.; Écija, D.; Seufert, K.; Auwärter, W.; Aurisicchio, C.; Fabbro, C.; Bonifazi, D.; Barth, J. V. Self-Assembly of Flexible One-Dimensional Coordination Polymers on Metal Surfaces. *J. Am. Chem. Soc.* **2010**, *132*, 6783–6790.

(12) Heim, D.; Seufert, K.; Auwärter, W.; Aurisicchio, C.; Fabbro, C.; Bonifazi, D.; Barth, J. V. Surface-Assisted Assembly of Discrete Porphyrin-Based Cyclic Supramolecules. *Nano Lett.* **2010**, *10*, 122–128.

(13) Haq, S.; Hanke, F.; Dyer, M. S.; Persson, M.; Iavicoli, P.; Amabilino, D. B.; Raval, R. Clean Coupling of Unfunctionalized Porphyrins at Surfaces to Give Highly Oriented Organometallic Oligomers. *J. Am. Chem. Soc.* **2011**, *133*, 12031–12039.

(14) Pham, T. A.; Song, F.; Alberti, M. N.; Nguyen, M.-T.; Trapp, N.; Thilgen, C.; Diederich, F.; Stöhr, M. Heat-Induced Formation of One-Dimensional Coordination Polymers on Au(111): An STM Study. *Chem. Commun.* **2015**, *51*, 14473–14476.

(15) Venkataraman, L.; Klare, J. E.; Tam, I. W.; Nuckolls, C.; Hybertsen, M. S.; Steigerwald, M. L. Single-Molecule Circuits with Well-Defined Molecular Conductance. *Nano Lett.* **2006**, *6*, 458–462.

(16) Dri, C.; Fronzoni, G.; Balducci, G.; Furlan, S.; Stener, M.; Feng, Z.; Comelli, G.; Castellarin-Cudia, C.; Cvetko, D.; Kladnik, G.; et al. Chemistry of the Methylamine Termination at a Gold Surface: From Autorecognition to Condensation. *J. Phys. Chem. C* **2016**, *120*, 6104–6115.

(17) Balducci, G.; Romeo, M.; Stener, M.; Fronzoni, G.; Cvetko, D.; Cossaro, A.; Dell'Angela, M.; Kladnik, G.; Venkataraman, L.; Morgante, A. Computational Study of Amino Mediated Molecular Interaction Evidenced in N 1s NEXAFS: 1,4-Diaminobenzene on Au (111). *J. Phys. Chem. C* **2015**, *119*, 1988–1995.

(18) Venkataraman, L.; Klare, J. E.; Nuckolls, C.; Hybertsen, M. S.; Steigerwald, M. L. Dependence of Single-Molecule Junction Conductance on Molecular Conformation. *Nature* **2006**, *442*, 904–907.

(19) Quinn, J. R.; Foss, F. W.; Venkataraman, L.; Hybertsen, M. S.; Breslow, R. Single-Molecule Junction Conductance through Diaminoacenes. *J. Am. Chem. Soc.* **2007**, *129*, 6714–6715.

(20) Kladnik, G.; Cvetko, D.; Batra, A.; Dell'Angela, M.; Cossaro, A.; Kamenetska, M.; Venkataraman, L.; Morgante, A. Ultrafast Charge Transfer through Noncovalent Au-N Interactions in Molecular Systems. *J. Phys. Chem. C* **2013**, *117*, 16477–16482.

(21) Cossaro, A.; Cvetko, D.; Floreano, L. Amino-Carboxylic Recognition on Surfaces: From 2D to 2D + 1 Nano-Architectures. *Phys. Chem. Chem. Phys.* **2012**, *14*, 13154–13162.

(22) Kladnik, G.; Puppin, M.; Coreno, M.; de Simone, M.; Floreano, L.; Verdini, A.; Morgante, A.; Cvetko, D.; Cossaro, A. Ultrafast Charge Transfer Pathways Through A Prototype Amino-Carboxylic Molecular Junction. *Nano Lett.* **2016**, *16*, 1955–1959.

(23) Feng, Z.; Castellarin Cudia, C.; Floreano, L.; Morgante, A.; Comelli, G.; Dri, C.; Cossaro, A. A Competitive Amino-Carboxylic Hydrogen Bond on a Gold Surface. *Chem. Commun.* **2015**, *51*, 5739–5742.

(24) Giannozzi, P.; Baroni, S.; Bonini, N.; Calandra, M.; Car, R.; Cavazzoni, C.; Ceresoli, D.;

Chiarotti, G. L.; Cococcioni, M.; Dabo, I.; et al. QUANTUM ESPRESSO: A Modular and Open-Source Software Project for Quantum Simulations of Materials. *J. Phys. Condens. Matter* **2009**, *21*, 395502.

(25) Perdew, J. P.; Burke, K.; Ernzerhof, M. Generalized Gradient Approximation Made Simple. *Phys. Rev. Lett.* **1996**, *77*, 3865–3868.

(26) Vanderbilt, D. Soft Self-Consistent Pseudopotentials in a Generalized Eigenvalue Formalism. *Phys. Rev. B* **1990**, *41*, 7892–7895.

(27) Grimme, S. Semiempirical GGA-Type Density Functional Constructed with a Long-Range Dispersion Correction. *J. Comput. Chem.* **2006**, *27*, 1787–1799.

(28) Barone, V.; Casarin, M.; Forrer, D.; Pavone, M.; Sambi, M.; Vittadini, A. Role and Effective Treatment of Dispersive Forces in Materials: Polyethylene and Graphite Crystals as Test Cases. *J. Comput. Chem.* **2009**, *30*, 934–939.

(29) Feng, Z.; Velari, S.; Cossaro, A.; Castellarin-Cudia, C.; Verdini, A.; Vesselli, E.; Dri, C.; Peressi, M.; De Vita, A.; Comelli, G. Trapping of Charged Gold Adatoms by Dimethyl Sulfoxide on a Gold Surface. *ACS Nano* **2015**, *9*, 8697–8709.

(30) Tersoff, J.; Hamann, D. R. Theory of the Scanning Tunneling Microscope. *Phys. Rev. B* **1985**, *31*, 805–813.

(31) Barth, J. V. V.; Brune, H.; Ertl, G.; Behm, R. J. Scanning Tunneling Microscopy Observations on the Reconstructed Au(111) Surface: Atomic Structure, Long-Range Superstructure, Rotational Domains, and Surface Defects. *Phys. Rev. B* **1990**, *42*, 9307–9318.

(32) Seufert, K.; Bocquet, M.-L.; Auwärter, W.; Weber-Bargioni, A.; Reichert, J.; Lorente, N.; Barth, J. V. Cis-Dicarbonyl Binding at Cobalt and Iron Porphyrins with Saddle-Shape Conformation. *Nat. Chem.* **2011**, *3*, 114–119.

(33) Yokoyama, T.; Yokoyama, S.; Kamikado, T.; Mashiko, S. Nonplanar Adsorption and Orientational Ordering of Porphyrin Molecules on Au(111). *J. Chem. Phys.* **2001**, *115*, 3814–3818.

(34) Scudiero, L.; Barlow, D. E.; Hipps, K. W. Physical Properties and Metal Ion Specific Scanning Tunneling Microscopy Images of Metal(II) Tetraphenylporphyrins Deposited from Vapor onto Gold (111). *J. Phys. Chem. B* **2000**, *104*, 11899–11905.

(35) Moresco, F.; Meyer, G.; Rieder, K.-H.; Ping, J.; Tang, H.; Joachim, C. TBPP Molecules on Copper Surfaces: A Low Temperature Scanning Tunneling Microscope Investigation. *Surf. Sci.* **2002**, *499*, 94–102.

(36) Auwärter, W.; Weber-Bargioni, A.; Riemann, A.; Schiffrin, A.; Gröning, O.; Fasel, R.; Barth, J. V. Self-Assembly and Conformation of Tetrapyridyl-Porphyrin Molecules on Ag(111). *J. Chem. Phys.* **2006**, *124*, 194708.

(37) Mielke, J.; Hanke, F.; Peters, M. V.; Hecht, S.; Persson, M.; Grill, L. Adatoms underneath Single Porphyrin Molecules on Au(111). *J. Am. Chem. Soc.* **2015**, *137*, 1844–1849.

(38) Maksymovych, P.; Voznyy, O.; Dougherty, D. B.; Sorescu, D. C.; Yates, J. T. Gold Adatom as a Key Structural Component in Self-Assembled Monolayers of Organosulfur Molecules on Au(111). *Prog. Surf. Sci.* **2010**, *85*, 206–240.

(39) Stoltze, P. Simulation of Surface Defects. *J. Phys. Condens. Matter* **1994**, *6*, 9495–9517.

(40) Zhang, J.-M.; Song, X.-L.; Zhang, X.-J.; Xu, K.-W.; Ji, V. Atomistic Simulation of Point Defects at Low-Index Surfaces of Noble Metals. *Surf. Sci.* **2006**, *600*, 1277–1282.

(41) Faraggi, M. N.; Jiang, N.; Gonzalez-Lakunza, N.; Langner, A.; Stepanow, S.; Kern, K.; Arnau, A. Bonding and Charge Transfer in Metal–Organic Coordination Networks on Au(111) with Strong Acceptor Molecules. *J. Phys. Chem. C* **2012**, *116*, 24558–24565.

(42) Yang, Z.; Corso, M.; Robles, R.; Lotze, C.; Fitzner, R.; Mena-Osteritz, E.; Bäuerle, P.; Franke, K. J.; Pascual, J. I. Orbital Redistribution in Molecular Nanostructures Mediated by Metal–Organic Bonds. *ACS Nano* **2014**, *8*, 10715–10722.

(43) Boscoboinik, J. A.; Calaza, F. C.; Habeeb, Z.; Bennett, D. W.; Stacchiola, D. J.; Purino, M. A.; Tysoe, W. T. One-Dimensional Supramolecular Surface Structures: 1,4-Diisocyanobenzene on Au(111) Surfaces. *Phys. Chem. Chem. Phys.* **2010**, *12*, 11624–11629.

(44) Meyer, J.; Nickel, A.; Ohmann, R.; Lokamani, L.; Toher, C.; Ryndyk, D. A.; Garmshausen, Y.; Hecht, S.; Moresco, F.; Cuniberti, G. Tuning the Formation of Discrete Coordination Nanostructures. *Chem. Commun.* **2015**, *51*, 12621–12624.

(45) Jewell, A. D.; Tierney, H. L.; Zenasni, O.; Lee, T. R.; Sykes, E. C. H. Asymmetric Thioethers as Building Blocks for Chiral Monolayers. *Top. Catal.* **2011**, *54*, 1357–1367.

(46) Bellisario, D. O.; Jewell, A. D.; Tierney, H. L.; Baber, A. E.; Sykes, E. C. H. Adsorption, Assembly, and Dynamics of Dibutyl Sulfide on Au{111}. *J. Phys. Chem. C* **2010**, *114*, 14583–14589.

(47) Pham, V. D.; Repain, V.; Chacon, C.; Bellec, A.; Girard, Y.; Rousset, S.; Abad, E.; Dappe, Y. J.; Smogunov, A.; Lagoute, J. Tuning the Electronic and Dynamical Properties of a Molecule by Atom Trapping Chemistry. *ACS Nano* **2017**, *11*, 10742–10749.

(48) Groom, C. R.; Bruno, I. J.; Lightfoot, M. P.; Ward, S. C. The Cambridge Structural Database. *Acta Crystallogr. Sect. B Struct. Sci. Cryst. Eng. Mater.* **2016**, *72*, 171–179.

(49) Klappenberger, F.; Weber-Bargioni, A.; Auwärter, W.; Marschall, M.; Schiffrin, A.; Barth, J. V. Temperature Dependence of Conformation, Chemical State, and Metal-Directed Assembly of Tetrapyridyl-Porphyrin on Cu(111). *J. Chem. Phys.* **2008**, *129*, 214702.

(50) Röckert, M.; Franke, M.; Tariq, Q.; Ditze, S.; Stark, M.; Uffinger, P.; Wechsler, D.; Singh, U.; Xiao, J.; Marbach, H.; et al. Coverage- and Temperature-Dependent Metalation and Dehydrogenation of Tetraphenylporphyrin on Cu(111). *Chemistry* **2014**, *20*, 8948–8953.

(51) Bürker, C.; Franco-Cañellas, A.; Broch, K.; Lee, T.-L.; Gerlach, A.; Schreiber, F. Self-Metalation of 2 H -Tetraphenylporphyrin on Cu(111) Studied with XSW: Influence of the Central Metal Atom on the Adsorption Distance. *J. Phys. Chem. C* **2014**, *118*, 13659–13666.

(52) González-Moreno, R.; Sánchez-Sánchez, C.; Trelka, M.; Otero, R.; Cossaro, A.; Verdini, A.; Floreano, L.; Ruiz-Bermejo, M.; García-Lekue, A.; Martín-Gago, J. A.; et al. Following the Metalation Process of Protoporphyrin IX with Metal Substrate Atoms at Room Temperature. *J. Phys. Chem. C* **2011**, *115*, 6849–6854.

(53) Goldoni, A.; Pignedoli, C. A.; Di Santo, G.; Castellarin-Cudia, C.; Magnano, E.; Bondino, F.; Verdini, A.; Passerone, D. Room Temperature Metalation of 2H-TPP Monolayer on Iron and Nickel Surfaces by Picking up Substrate Metal Atoms. *ACS Nano* **2012**, *6*, 10800–10807.

(54) Diller, K.; Klappenberger, F.; Marschall, M.; Hermann, K.; Nefedov, A.; Wöll, C.; Barth, J. V. Self-Metalation of 2H-Tetraphenylporphyrin on Cu(111): An x-Ray Spectroscopy Study. *J. Chem. Phys.* **2012**, *136*, 014705.

(55) Chen, M.; Feng, X.; Zhang, L.; Ju, H.; Xu, Q.; Zhu, J.; Gottfried, J. M.; Ibrahim, K.; Qian, H.; Wang, J. Direct Synthesis of Nickel(II) Tetraphenylporphyrin and Its Interaction with a Au(111) Surface: A Comprehensive Study. *J. Phys. Chem. C* **2010**, *114*, 9908–9916.

(56) Papageorgiou, A. C.; Fischer, S.; Oh, S. C.; Sağlam, O.; Reichert, J.; Wiengarten, A.; Seufert, K.; Vijayaraghavan, S.; Ecija, D.; Auwärter, W.; et al. Self-Terminating Protocol for an Interfacial Complexation Reaction in Vacuo by Metal-Organic Chemical Vapor Deposition. *ACS Nano* **2013**, *7*, 4520–4526.

(57) Di Santo, G.; Castellarin-Cudia, C.; Fanetti, M.; Taleatu, B.; Borghetti, P.; Sangaletti, L.; Floreano, L.; Magnano, E.; Bondino, F.; Goldoni, A. Conformational Adaptation and Electronic Structure of 2H-Tetraphenylporphyrin on Ag(111) during Fe Metalation. *J. Phys. Chem. C* **2011**, *115*, 4155–4162.

(58) Bischoff, F.; Seufert, K.; Auwärter, W.; Seitsonen, A. P.; Heim, D.; Barth, J. V. Metalation of Porphyrins by Lanthanide Atoms at Interfaces: Direct Observation and Stimulation of Cerium Coordination to 2H-TPP/Ag(111). *J. Phys. Chem. C* **2018**, *122*, 5083–5092.

(59) Esch, F.; Dri, C.; Spessot, A.; Africh, C.; Cautero, G.; Giuressi, D.; Sergo, R.; Tommasini, R.; Comelli, G. The FAST Module: An Add-on Unit for Driving Commercial Scanning Probe Microscopes at Video Rate and Beyond. *Rev. Sci. Instrum.* **2011**, *82*, 053702.

(60) Dri, C.; Esch, F.; Africh, C.; Comelli, G. How to Select Fast Scanning Frequencies for High-Resolution Fast STM Measurements with a Conventional Microscope. *Meas. Sci. Technol.* **2012**, *23*, 055402.

(61) Patera, L. L.; Bianchini, F.; Africh, C.; Dri, C.; Soldano, G.; Mariscal, M. M.; Peressi, M.; Comelli, G. Real-Time Imaging of Adatom-Promoted Graphene Growth on Nickel. *Science* **2018**, *359*, 1243–1246.

(62) Mielke, J.; Martínez-Blanco, J.; Peters, M. V.; Hecht, S.; Grill, L. Observing Single-Atom Diffusion at a Molecule-Metal Interface. *Phys. Rev. B* **2016**, *94*, 035416.

(63) Lepper, M.; Köbl, J.; Zhang, L.; Meusel, M.; Hölzel, H.; Lungerich, D.; Jux, N.; de Siervo, A.; Meyer, B.; Steinrück, H.-P.; et al. Controlling the Self-Metalation Rate of Tetraphenylporphyrins on Cu(111) via Cyano Functionalization. *Angew. Chemie Int. Ed.* **2018**, *57*, 10074–10079.

(64) Liljeroth, P.; Repp, J.; Meyer, G. Current-Induced Hydrogen Tautomerization and Conductance Switching of Naphthalocyanine Molecules. *Science* **2007**, *317*, 1203–1206.

(65) Auwärter, W.; Seufert, K.; Bischoff, F.; Ecija, D.; Vijayaraghavan, S.; Joshi, S.; Klappenberger, F.; Samudrala, N.; Barth, J. V. A Surface-Anchored Molecular Four-Level Conductance Switch Based on Single Proton Transfer. *Nat. Nanotechnol.* **2011**, *7*, 41–46.

(66) Di Santo, G.; Blankenburg, S.; Castellarin-Cudia, C.; Fanetti, M.; Borghetti, P.; Sangaletti, L.; Floreano, L.; Verdini, A.; Magnano, E.; Bondino, F.; et al. Supramolecular Engineering through Temperature-Induced Chemical Modification of 2H-Tetraphenylporphyrin on Ag(111): Flat Phenyl Conformation and Possible Dehydrogenation Reactions. *Chem. - A Eur. J.* **2011**, *17*, 14354–14359.

TOC Graphic